Geological Survey of Canada

CURRENT RESEARCH
2005-F2

U-Pb ages from the northern Wecho River area, southwestern Slave Province, Northwest Territories: constraints on late Archean plutonism and metamorphism

L. Ootes, S. Buse, W.J. Davis, and B. Cousens

2005

Natural Resources Canada Ressources naturelles Canada

Canada

CURRENT RESEARCH

ISSN 1701-4387
Catalogue No. M44-2005/F2E-PDF
ISBN 0-662-40226-X

A copy of this publication is also available for reference by depository libraries across Canada through access to the Depository Services Program's website at http://dsp-psd.pwgsc.gc.ca

A free digital download of this publication is available from the Geological Survey of Canada Bookstore web site:

http://gsc.nrcan.gc.ca/bookstore/

Click on Free Download.

Authors' addresses

L. Ootes (Luke_ootes@gov.nt.ca)
Northwest Territories Geoscience Office
Box 1500
Yellowknife, NT X1A 2R3

S. Buse (sbuse@connect.carleton.ca)
B. Cousens(bcousens@css.carleton.ca)
Carleton University
2240 Herzberg Laboratories
1125 Colonel By Drive
Ottawa, ON K1S 5B6

W.J. Davis (bidavis@nrcan.gc.ca)
Continental Geoscience Division
Geological Survey of Canada
601 Booth Street
Ottawa, Ontario K1A 0E8

Publication approved by Continental Geoscience Division

Original manuscript submitted: 2004-03-11

Final version approved for publication: 2004-04-13

U-Pb ages from the northern Wecho River area, southwestern Slave Province, Northwest Territories: constraints on late Archean plutonism and metamorphism

L. Ootes, S. Buse, W.J. Davis, and B. Cousens

Ootes, L., Buse, S., Davis, W.J., and Cousens, B., 2005: U-Pb ages from the northern Wecho River area, southwestern Slave Province, Northwest Territories: constraints on late Archean plutonism and metamorphism; Geological Survey of Canada, Current Research 2005-F2, 13 p.

Abstract: New U-Pb thermal-ionization mass spectrometry (TIMS) and Sensitive High Resolution Ion Micro Probe (SHRIMP) ages from four granitoid plutons place constraints on the timing of plutonism and metamorphism in the Wecho River area in the southwestern Slave Craton. U-Pb monazite ages show that the Hickey pluton crystallized at 2600.6 ± 2.1 Ma, prior to, or early during, granulite-grade metamorphism. All zircons analyzed from the Hickey pluton are older than 2855 Ma and are interpreted as being inherited from Mesoarchean basement. The Dauphinee pluton is an orthopyroxene-bearing tonalite and crystallized at 2590 ± 2.3 Ma during granulite-grade metamorphism. This age is within error of other orthopyroxene-bearing granites in neighbouring areas, indicative of widespread granulite-grade metamorphism at 2590 Ma. The Armi pluton crystallized at 2600 ± 5 Ma. The crystallization age constrains upper-amphibolite-grade metamorphism in the Armi Lake supracrustal belt to younger than 2600 Ma. The Wecho pluton crystallized at 2590 ± 8 Ma, restricting the latest pulses of magmatism in the area to before 2590 Ma.

Résumé : De nouveaux âges U-Pb obtenus pour quatre plutons granitoïdes par spectrométrie de masse à thermo-ionisation (TIMS) et par analyse à la microsonde ionique à haute résolution et à haut niveau de sensibilité (microsonde SHRIMP) permettent d'encadrer l'âge du plutonisme et du métamorphisme dans la région de la rivière Wecho, dans le sud-ouest du craton des Esclaves. La datation U-Pb de la monazite indique que la cristallisation du pluton de Hickey remonte à 2600,6 ± 2,1 Ma, soit avant le métamorphisme au faciès des granulites ou au début de celui-ci. Tous les zircons analysés qui proviennent du pluton de Hickey ont plus de 2855 Ma et sont interprétés comme étant hérités du socle méso-archéen. Le pluton de Dauphinee est une tonalite à orthopyroxène dont la cristallisation remonte à 2590 ± 2,3 Ma, soit pendant le métamorphisme au faciès des granulites. Cet âge est à l'intérieur de la marge d'erreur pour d'autres granites à orthopyroxène de régions avoisinantes, ce qui atteste un métamorphisme au faciès des granulites répandu à 2590 Ma. La cristallisation du pluton d'Armi remonte à 2600 ± 5 Ma; d'après cet âge, le métamorphisme au faciès supérieur des amphibolites survenu dans la zone supracrustale d'Armi Lake doit dater de moins de 2600 Ma. La cristallisation du pluton de Wecho remonte à 2590 ± 8 Ma, et les plus récents événements magmatiques dans la région ont donc plus de 2590 Ma.

INTRODUCTION

The Slave Structural Province is a well exposed Archean craton in the northwestern Canadian Shield. It is composed of 2.73 to 2.63 Ga supracrustal sequences that are extensively intruded by approximately 2.63 to 2.58 Ga Archean granitoid bodies (Fig.1; Padgham and Fyson, 1992; Bleeker and Davis, 1999; Davis and Bleeker, 1999). Mesoarchean basement (>2.85 Ga) is locally preserved in the western and central part of the structural province and underlies a thin cover sequence of quartzite and iron-formation, and thick, approximately 2.7 Ga basalts that occur in the south through to the north-western part of the craton (Fig. 1; Bleeker et al., 1999). Radiogenic isotopes in granitoid rocks trace the eastern subsurface extent of the basement sequence (i.e. Pb-Pb, Sm-Nd, U-Pb; Thorpe et al., 1992; Davis and Hegner, 1992; Davis et al., 1996; MacLachlan et al., 2002); however, to the southwest, the subsurface extent of basement is poorly constrained (Yamashita et al., 1999). Similarly, the timing of deformation and metamorphism east of Yellowknife has been well constrained by U-Pb zircon dating (Davis and Bleeker, 1999), but to the northwest it is only regionally correlated to similar sequences.

The northern Wecho River area is 150 km north-north-west of Yellowknife, Northwest Territories, and was the focus of a two-year (2003–2004) bedrock-mapping project (Fig. 1). The bedrock geology of the Wecho River area was first documented by Yardley (1949) and has since received negligible attention. In contrast, most of the southwestern Slave Province has had modern 1:50 000-scale bedrock mapping and subsequent larger scale compilations that integrate geochemical, geochronological, and mineral-deposit studies (Henderson, 1985, 2004; Stubley, 1997; Pehrsson, 2002; Jackson, 2003). The Wecho River bedrock-mapping project

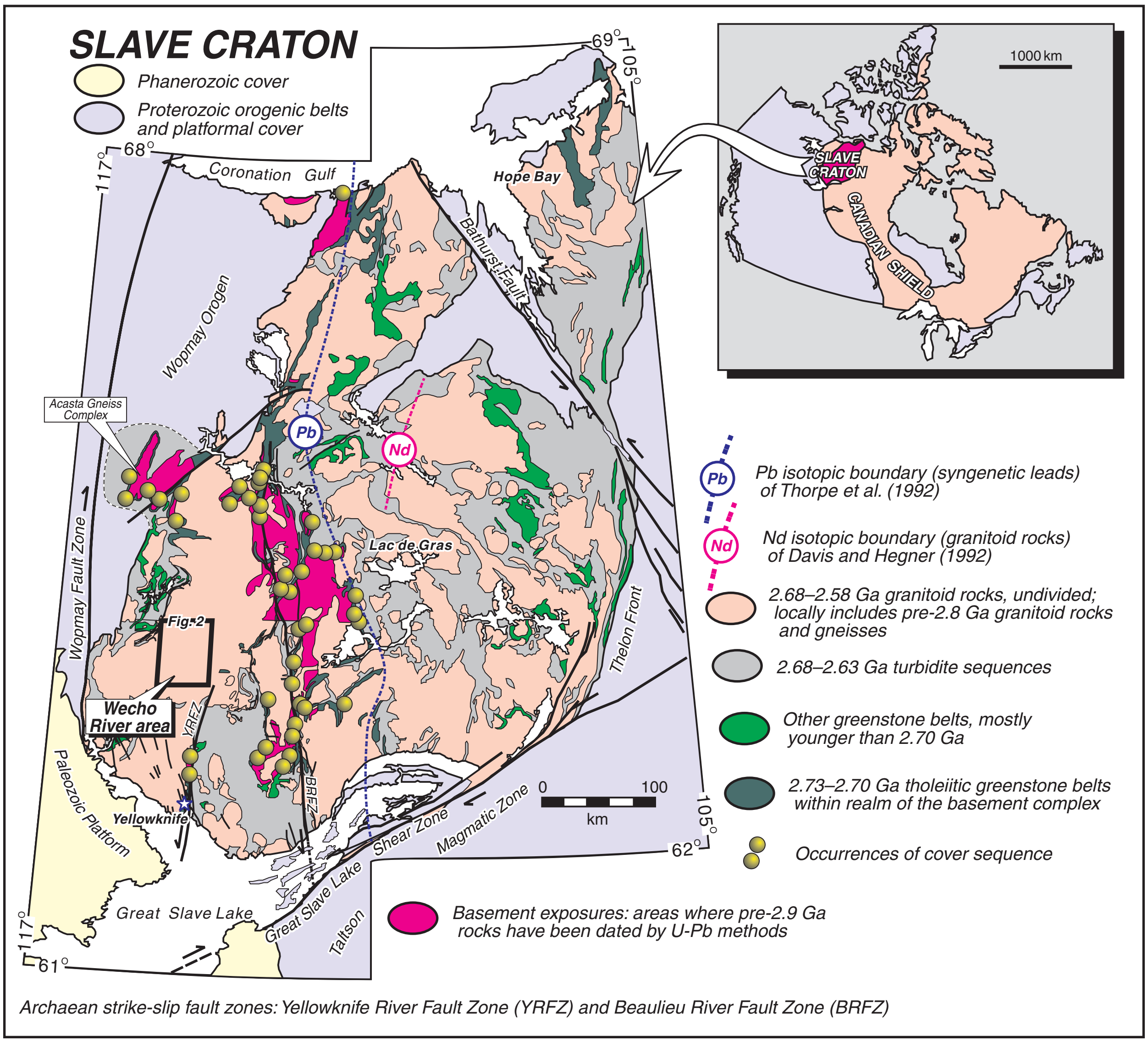

Figure 1. *Geology of the Slave Craton. Northern part of the Wecho River area is identified. Modified after Bleeker and Davis (1999).*

was initiated to update the geology and use integrated studies to compare and contrast the geology with neighbouring areas in the southwestern part of the Slave Craton. In this paper new U-Pb age data for four granitoid suites are reported that place constraints on the timing of plutonism and metamorphism in the Wecho River area.

REGIONAL GEOLOGY

Fieldwork in 2003 focused on the northern part of the area, which comprises NTS 85-O/09, 10, 15, and 16 (Fig. 2). An overview of the geology from the 2003 fieldwork is presented below.

Supracrustal rocks

The supracrustal rocks in the study area consist of middle-amphibolite- to granulite-grade pelite and psammite with lesser amounts of amphibolite and mafic granulite. Various granitoid rocks intrude all supracrustal rocks in the area. The newly identified Armi Lake supracrustal belt (Fig. 2; Ootes, 2004) occurs in the southern part of the study area. Pelitic rocks in this belt are biotite+sillimanite (commonly overgrowing cordierite)+melt-bearing and depositional features are generally obliterated. Psammitic rocks are locally melt-bearing, but to a lesser extent than the pelite, and bedding is generally preserved. Early foliations (S_1/S_2) are locally preserved, but the main foliation in the area is defined by melt and sillimanite (S_2/S_3). Both the early and main foliations are cut by a late crenulation cleavage (S_3/S_4), defined by biotite±muscovite.

The supracrustal rocks in the northern part of the study area are upper amphibolite to granulite facies and consist of metatexite, diatexite, and mafic granulite (Fig. 2; Ootes, 2004). Diagnostic mineral assemblages in the pelitic rocks consist of biotite+sillimanite±K-feldspar±cordierite±garnet±spinel. Amphibolite and mafic granulite rocks are rare, but where they occur, diagnostic mineral assemblages include hornblende in subgranulite-grade rocks, and orthopyroxene in granulite-grade rocks. Melt and gneissic layering define the foliation in these high-grade rocks, which is tentatively correlated with the S_2/S_3 foliation in the Armi Lake belt in the south.

Intrusive Rocks

Based on crosscutting relationships, deformation state, mineralogy, and enclave composition, the granitoid rocks in the study area were divided into four units (Fig. 2). These include 1) the Hickey pluton, a strongly deformed granite to granodiorite, which occurs in the northern and southern part of the study area; 2) the Dauphinee pluton, an orthopyroxene-bearing granodiorite to mafic granulite; 3) the Armi pluton, a biotite-granodiorite that extensively intrudes the Armi Lake supracrustal rocks; and 4) the Wecho pluton, a K-feldspar- porphyritic granite that is texturally and mineralogically similar to the Stagg Suite to the south (Henderson, 1985). The crystallization age of each of these units will help constrain the timing of metamorphism and deformation of the supracrustal rocks.

GEOCHRONOLOGY

Analytical techniques

Samples were prepared and analyzed at the Geological Survey of Canada in Ottawa. Heavy mineral concentrates of each sample were prepared through crushing, grinding, Wilfley™ table and heavy liquid separation. Grains were then sorted using the Frantz™ isodynamic separator by magnetic susceptibility. Zircons and monazites were then optically sorted and separated into fractions, defined by morphology. For TIMS analyses, all zircon were air abraded. Analytical methods for U-Pb analyses of zircon and monazite are summarized in Roddick et al. (1987) and Parrish et al. (1987). Analytical errors are determined based on error propagation methods of Roddick (1987). A modified (York, 1969) regression method was used to calculate upper and lower concordia intercept ages and Isoplot v. 3.00 (Ludwig, 2003) was used to calculated weighted mean ages. TIMS analytical results are presented in Table 1.

Analytical procedures for U-Pb zircon analyses using the SHRIMP II at the Geological Survey of Canada followed those described by Stern (1997), with standards and U-Pb calibration methods following Stern and Amelin (2003). Zircons were cast in 2.5 cm diameter epoxy mounts (GSC #318) along with fragments of the GSC laboratory standard zircon (z6266, with $^{206}Pb/^{238}U$ age = 559 Ma). The internal features of the zircons were imaged by SEM in backscattered electron (BSE) mode prior to analyses. Analyses were conducted using an $^{16}O^-$ primary beam. Two different sized spots were used for analysis, one ca. 15 µm in diameter, and another ca. 9 µm in diameter with a beam current of ca. 3.5 and 1nA respectively. The 1σ external errors of Pb/U ratios incorporate a ±1.0 % error in the standard calibration. Isoplot v. 3.00 (Ludwig, 2003) was used to generate concordia plots and calculate weighted means. SHRIMP analytical results are presented in Table 2 and a summary of ages is in Table 3.

Hickey pluton — biotite-magnetite granite (sample #03sb028 — lab #z7992)

Unit Description

A sample of the Hickey pluton was collected to constrain the maximum age of granulite-grade metamorphism in the area, to place this major map unit in temporal context with similar plutonic units in the southwestern Slave Craton, and to determine if the pluton interacted with Mesoarchean basement during ascent. The biotite-magnetite-bearing pluton occurs in the northern part of the study area (Fig. 2) and ranges from granite to granodiorite. It is recrystallized and strongly deformed to gneiss in places, with a foliation defined by biotite and quartz (Fig. 3a, b). It is locally plagioclase-phyric

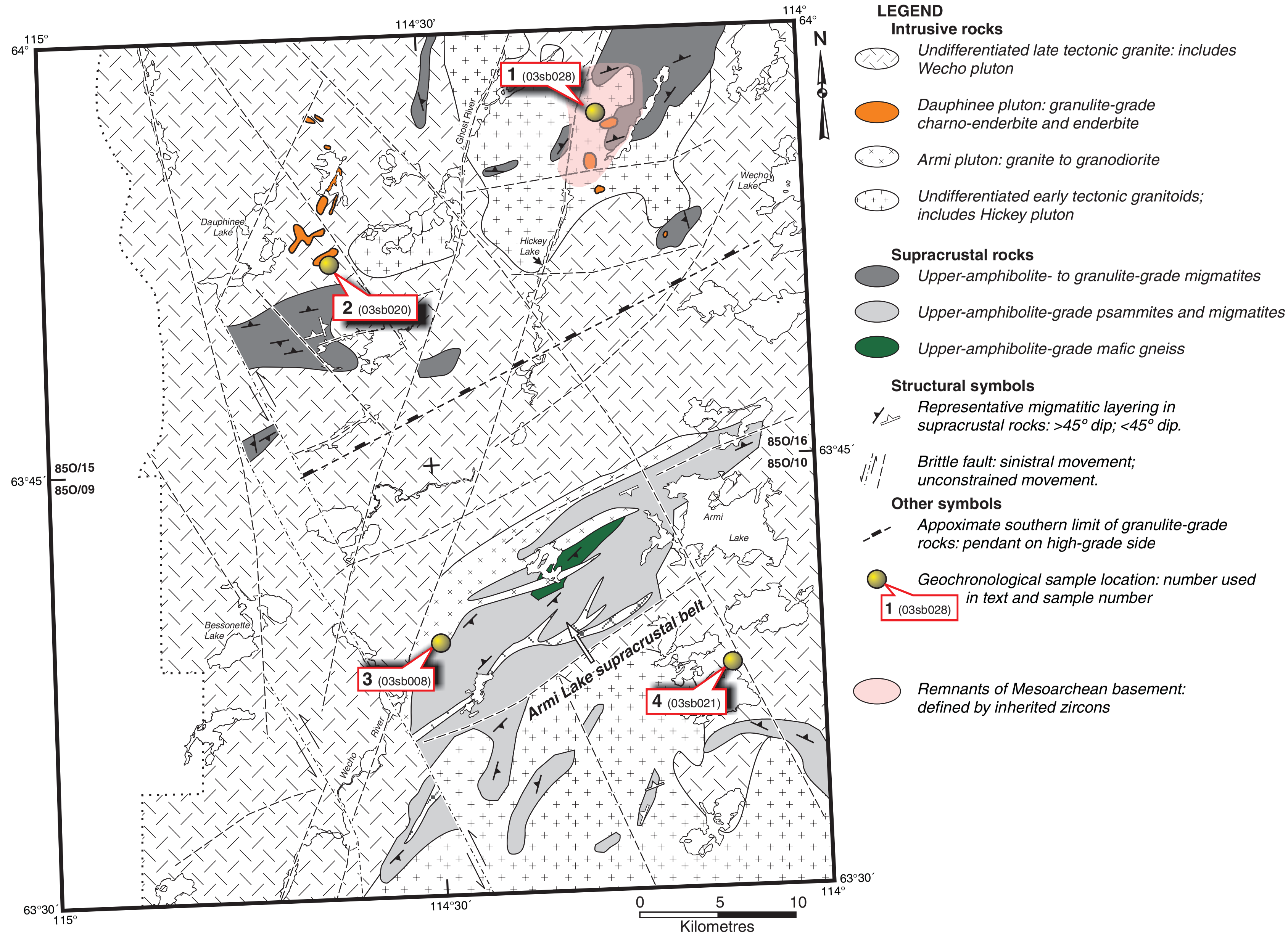

Figure 2. Simplified geology of the northern part of the Wecho River area. Location is identified in Figure 1. Modified after Ootes (2004).

Table 1. U-Pb analytical data — Thermal ionization mass spectrometry.

																		Apparent ages (Ma)[4]			
Fraction	Description[1]	# grains	Size (µm)	Wt. (µg)	U[2] (ppm)	Pb*[2] (ppm)	^{206}Pb[3]/^{204}Pb	Pbc[2] (pg)	^{208}Pb[3]/^{206}Pb	^{207}Pb[3]/^{235}U	±^{207}Pb/^{235}U	^{206}Pb[3]/^{238}U	±^{206}Pb/^{238}U	Corr coeff.	^{207}Pb[3]/^{206}Pb	±^{207}Pb/^{206}Pb	^{206}Pb/^{238}U	±^{206}Pb/^{238}U	^{207}Pb/^{206}Pb	±^{207}Pb/^{206}Pb	Disc. (%)
03sb008A (Z7988)																					
M1A (M)	pY,Clr,fFr,Sub,NAbr,M-0.5A	1	125	1	1840	21813	8946	6	27.20	11.395	0.013	0.4819	0.0004	0.9388	0.17149	0.00007	2535.6	3.7	2572.2	1.4	1.7
M2A (M)	pY,Alt,Sub,NAbr,M-0.5A	1	125	1	2912	14344	20395	4	10.42	11.632	0.013	0.4903	0.0004	0.9454	0.17207	0.00007	2572.0	3.7	2577.8	1.4	0.3
M3A (M)	Y,Alt,Sub,NAbr,M-0.5A	1	200	1	3683	40187	16817	7	24.67	11.485	0.013	0.4871	0.0004	0.9412	0.17101	0.00007	2558.1	3.7	2567.6	1.4	0.5
M4A (M)	Y,Alt,An,NAbr,M-0.5A	1	150	1	2792	13737	18249	5	10.38	11.676	0.013	0.4915	0.0004	0.9409	0.17231	0.00007	2577.0	3.7	2580.2	1.4	0.2
Z1 (Z)	B.Alt.fFr.E.Pr.Abr.M0°	1	130	1	496	308	4840	5	0.10	16.163	0.018	0.5495	0.0005	0.9407	0.21335	0.00009	2822.9	4.1	2931.2	1.4	4.6
Z2 (Z)	pBr.Clr.fFr.cln.Pr.Abr.M0°	2	77	1	462	252	1446	9	0.14	11.506	0.016	0.4843	0.0005	0.8923	0.17232	0.00011	2545.8	4.4	2580.3	2.2	1.6
Z3 (Z)	Br.fFr.St.Abr.M0°	1	87	1	586	294	2613	6	0.05	11.463	0.014	0.4794	0.0005	0.9200	0.17341	0.00009	2524.7	4.0	2590.9	1.7	3.1
03sb020A (Z7990)																					
Z1A (Z)	pBr Clr fFr El Abr M1°	1	81	2	231	125	3273	4	0.11	11.770	0.015	0.4922	0.0005	0.9185	0.17342	0.00009	2580.3	4.4	2590.9	1.7	0.5
Z1B (Z)	pBr.Clr.rFr.St.Abr.M1°	1	113	2	401	206	5628	4	0.05	11.588	0.014	0.4881	0.0005	0.9381	0.17219	0.00008	2562.5	3.9	2579.0	1.5	0.8
Z1C (Z)	pBr,Clr,St,Abr,M1°	2	98	2	484	256	3103	10	0.09	11.602	0.014	0.4882	0.0004	0.9187	0.17235	0.00009	2563.0	3.8	2580.6	1.7	0.8
Z2A (Z)	Br.Clr.fFr.Sub.Abr.M1°	1	214	7	402	211	10034	8	0.07	11.750	0.013	0.4917	0.0004	0.9429	0.17331	0.00007	2578.1	3.7	2589.8	1.4	0.6
Z2B (Z)	Br.Clr.fFr.Sub.Abr.M1°	1	214	9	307	160	8567	10	0.06	11.747	0.013	0.4918	0.0004	0.9436	0.17323	0.00007	2578.5	3.7	2589.1	1.4	0.5
03sb021A (Z7991)																					
M1 (M)	Co.Clr.Eu.NAbr.M-0.5A	1	100	1	14111	16796	96280	4	1.64	11.594	0.013	0.4896	0.0004	0.9452	0.17174	0.00007	2569.1	3.7	2574.6	1.4	0.3
M2 (M)	pY,Tb,Sub,NAbr,M-0.5A	1	100	1	9838	11661	83489	4	1.66	11.400	0.013	0.4842	0.0004	0.9450	0.17077	0.00007	2545.4	3.7	2565.2	1.4	0.9
M3 (M)	pY,Tb,fFr,Sub,NAbr,M-0.5A	1	150	1	10913	13135	72564	5	1.70	11.449	0.013	0.4847	0.0004	0.9455	0.17131	0.00007	2547.7	3.7	2570.5	1.4	1.1
Z1 (Z)	Co.Clr.rFr.El.Ro.Abr.M3°	1	80	1	144	72	1438	1	0.15	10.195	0.023	0.4396	0.0007	0.8861	0.16818	0.00020	2349.0	6.1	2539.6	3.9	8.9
Z2A (Z)	Co.Clr.Sub.Abr.M3°	1	100	4	64	40	1275	6	0.26	12.137	0.016	0.5107	0.0005	0.8677	0.17235	0.00012	2659.7	4.5	2580.6	2.3	-3.7
03sb028A (Z7992)																					
M1 (M)	Co.Clr.Eu.NAbr.M-0.5A	1	100	1	13576	52969	27850	15	7.92	11.917	0.013	0.4953	0.0004	0.9456	0.17451	0.00007	2593.5	3.8	2601.4	1.4	0.4
M3 (M)	Y,Tb,rFr,Sub,NAbr,M-0.5A	1	200	1	5697	26453	28957	6	9.62	11.933	0.014	0.4962	0.0005	0.9473	0.17444	0.00007	2597.2	3.9	2600.7	1.4	0.2
M4 (M)	Y,Clr,Sub,NAbr,M-0.5A	1	200	1	21255	69892	35851	18	6.49	11.905	0.013	0.4953	0.0004	0.9459	0.17433	0.00007	2593.4	3.8	2599.7	1.4	0.3
Z1A (Z)	Co,Clr,fFr,El,Pr,Abr,Dia	7	98	2	301	194	1379	17	0.18	15.219	0.019	0.5421	0.0005	0.8984	0.20362	0.00012	2792.2	4.3	2855.4	1.9	2.7
Z2 (Z)	pY,Clr,rFr,St,Abr,Dia	1	66	1	586	362	2224	5	0.07	16.172	0.023	0.5603	0.0007	0.9370	0.20934	0.00011	2867.8	5.8	2900.5	1.7	1.4
Z2 (Z)	pBr,Clr,St,Abr,Dia	1	66	1	582	395	440	17	0.19	16.081	0.052	0.5632	0.0020	0.9204	0.20710	0.00028	2879.6	16.3	2883.0	4.5	0.1
Z3 (Z)	Co,Clr,rFr,cln,Ro,Abr,Dia	4	57	2	63	42	903	4	0.13	17.287	0.034	0.5746	0.0010	0.8974	0.21822	0.00019	2926.5	8.5	2967.6	2.8	1.7
Z4 (Z)	Br,Clr,rFr,Ro,Abr,Dia	4	87	3	352	216	2964	12	0.08	15.969	0.019	0.5545	0.0005	0.9231	0.20888	0.00010	2843.8	4.2	2896.9	1.6	2.3

[1] Description: Z=zircon, M=monazite, Co=colourless, Br=brown, pBr=pale brown, Y=yellow, pY=pale yellow, Alt=altered, Clr=clear, Tb=turbid, fFr=few fractures, rFr=rare fractures, cln=clear inclusions, An=anhedral, El=elongate, Eu=euhedral, Pr=prismatic, Ro=rounded, St=stubby prism, Sub=subhedral, Abr=abraded, NAbr=not abraded

[2] Concentration uncertainty varies with sample weight: >10% for sample weights <10 µg, <10% for sample weights above 10 µg. * = radiogenic Pb. Pbc = total common Pb (picograms) analysis corrected for spike and fractionation.

[3] Atomic ratios corrected for spike, fractionation, blank and initial common Pb, except ^{206}Pb/^{20}4Pb ratio corrected for spike and fractionation only. Errors are one sigma absolute. Blank composition (atomic proportions): ^{208}Pb = 0.5197; ^{207}Pb=0.2136; ^{206}Pb=.2529; ^{204}Pb = .0139. Common Pb correction based on Cumming & Richards (1975) model.

[4] ^{206}Pb/^{238}U age and ^{207}Pb/^{206}Pb age with 2 S absolute error in Ma.

Table 2. U-Pb analytical data — SHRIMP.

Spot description	U (ppm)	Th (ppm)	Th/U	Pb* (ppm)	^{204}Pb (ppb)	$^{204}Pb/^{206}Pb$	± $^{204}Pb/^{206}Pb$	$f(206)^{204}$	$^{208}Pb/^{206}Pb$	± $^{208}Pb/^{206}Pb$	$^{207}Pb/^{235}U$	± $^{207}Pb/^{235}U$	$^{206}Pb/^{238}U$	± $^{206}Pb/^{238}U$	Corr coeff.	$^{207}Pb/^{206}Pb$	± $^{207}Pb/^{206}Pb$	Apparent ages $^{206}Pb/^{238}U$	Apparent ages ± $^{206}Pb/^{238}U$	Apparent ages $^{207}Pb/^{206}Pb$	Apparent ages ± $^{207}Pb/^{206}Pb$	% Discord
03sb008A (Z7988)																						
7988-166.1	295	3	0.01	147	9	0.00007	0.00002	0.00127	0.0025	0.0008	11.871	0.173	0.492	0.006	0.9024	0.17494	0.00111	2580	26	2605	11	1
7988-135.1	907	23	0.03	461	7	0.00002	0.00001	0.00032	0.0075	0.0004	12.035	0.135	0.501	0.005	0.9691	0.17435	0.00048	2617	23	2600	5	-0.6
7988-154.1	1022	330	0.33	562	4	0.00001	0.00001	0.00016	0.0943	0.0010	12.086	0.145	0.504	0.005	0.9255	0.17409	0.00080	2629	23	2597	8	-1.2
7988-163.1	613	200	0.34	355	3	0.00001	0.00001	0.00021	0.0953	0.0015	12.688	0.680	0.530	0.026	0.9615	0.17361	0.00258	2742	112	2593	25	-5.7
7988-140.1	890	474	0.55	506	5	0.00001	0.00001	0.00024	0.1512	0.0013	11.978	0.152	0.498	0.006	0.9657	0.17430	0.00058	2607	25	2599	6	-0.3
7988-135.2	210	114	0.56	121	10	0.00011	0.00005	0.00184	0.1551	0.0026	12.694	0.249	0.497	0.008	0.8887	0.18531	0.00168	2600	35	2701	15	3.7
7988-141.1	1019	689	0.70	589	51	0.00012	0.00002	0.00207	0.1955	0.0014	11.754	0.155	0.490	0.005	0.8823	0.17388	0.00109	2572	23	2595	10	0.9
7988-143.1	1008	777	0.80	586	22	0.00005	0.00001	0.00094	0.2302	0.0018	11.563	0.132	0.481	0.005	0.9499	0.17448	0.00063	2530	22	2601	6	2.7
7988-146.1	478	432	0.93	291	6	0.00003	0.00002	0.00053	0.2594	0.0032	11.917	0.175	0.492	0.006	0.8733	0.17557	0.00127	2581	25	2611	12	1.2
7988-155.1	488	620	1.31	342	12	0.00006	0.00001	0.00097	0.3718	0.0025	13.490	0.172	0.522	0.006	0.9208	0.18749	0.00094	2707	25	2720	8	0.5
03sb020A (Z7990)																						
7990-95.1	1595	554	0.36	941	10	0.00001	0.00000	0.00025	0.1030	0.0008	12.730	0.175	0.538	0.007	0.9839	0.17172	0.00043	2774	30	2575	4	-7.7
7990-110.1	474	125	0.27	254	8	0.00004	0.00001	0.00069	0.0765	0.0009	11.929	0.140	0.498	0.005	0.9481	0.17361	0.00066	2607	23	2593	6	-0.5
7990-109.1	828	36	0.04	418	3	0.00001	0.00001	0.00014	0.0132	0.0005	11.865	0.140	0.495	0.005	0.9663	0.17397	0.00053	2591	24	2596	5	0.2
7990-112.1	503	287	0.59	284	5	0.00002	0.00001	0.00040	0.1630	0.0012	11.639	0.157	0.492	0.006	0.9440	0.17175	0.00077	2577	26	2575	8	-0.1
7990-107.1	911	25	0.03	457	6	0.00002	0.00001	0.00026	0.0082	0.0003	11.819	0.154	0.494	0.006	0.9063	0.17359	0.00097	2587	24	2593	9	0.2
7990-119.1	1067	49	0.05	542	1	0.00000	0.00000	0.00003	0.0137	0.0002	11.910	0.147	0.497	0.006	0.9599	0.17368	0.00060	2602	24	2593	6	-0.3
7990-118.1	873	39	0.05	437	2	0.00000	0.00001	0.00008	0.0130	0.0005	11.766	0.139	0.491	0.005	0.9560	0.17390	0.00061	2574	23	2596	6	0.8
7990-120.1	369	111	0.31	192	6	0.00004	0.00002	0.00069	0.0851	0.0013	11.457	0.150	0.481	0.006	0.9392	0.17291	0.00078	2530	25	2586	8	2.2
7990-125.1	810	31	0.04	408	7	0.00002	0.00001	0.00034	0.0110	0.0003	11.817	0.144	0.494	0.006	0.9650	0.17343	0.00056	2589	24	2591	5	0.1
7990-127.1	992	164	0.17	518	2	0.00001	0.00001	0.00010	0.0439	0.0005	11.938	0.136	0.498	0.005	0.9739	0.17388	0.00045	2605	23	2595	4	-0.4
7990-115.1	674	71	0.11	342	14	0.00005	0.00001	0.00083	0.0296	0.0009	11.781	0.156	0.490	0.005	0.8894	0.17424	0.00106	2572	23	2599	10	1
7990-121.1	1527	902	0.61	898	6	0.00001	0.00000	0.00015	0.1709	0.0007	12.130	0.141	0.508	0.006	0.9655	0.17309	0.00053	2649	24	2588	5	-2.4
03sb021A (Z7991)																						
7991-44.1	697	11	0.02	353	23	0.00008	0.00002	0.00133	0.0045	0.0008	11.924	0.195	0.501	0.006	0.8553	0.17271	0.00147	2617	28	2584	14	-1.3
7991-60.1	491	8	0.02	248	9	0.00004	0.00002	0.00074	0.0062	0.0008	11.928	0.176	0.497	0.006	0.8330	0.17414	0.00143	2600	24	2598	14	-0.1
7991-46.1	1328	98	0.08	705	18	0.00003	0.00001	0.00053	0.0234	0.0005	12.353	0.226	0.515	0.007	0.8389	0.17383	0.00174	2680	31	2595	17	-3.3
7991-63.1	627	66	0.11	322	7	0.00003	0.00001	0.00046	0.0300	0.0005	11.887	0.157	0.495	0.006	0.8968	0.17403	0.00103	2594	24	2597	10	0.1
7991-51.1	513	59	0.12	248	23	0.00011	0.00004	0.00192	0.0344	0.0018	11.196	0.201	0.465	0.007	0.8984	0.17456	0.00139	2462	31	2602	13	5.4
7991-68.1	379	51	0.14	193	8	0.00005	0.00001	0.00091	0.0378	0.0008	11.608	0.156	0.490	0.006	0.9391	0.17197	0.00080	2569	25	2577	8	0.3
7991-48.1	647	117	0.19	336	3	0.00001	0.00001	0.00018	0.0537	0.0006	11.819	0.156	0.492	0.005	0.9016	0.17438	0.00100	2577	24	2600	10	0.9
7991-65.1	48	9	0.19	25	3	0.00016	0.00007	0.00281	0.0559	0.0034	12.275	0.325	0.485	0.010	0.8782	0.18347	0.00234	2550	46	2685	21	5
7991-66.1	861	232	0.28	471	7	0.00002	0.00001	0.00032	0.0767	0.0008	12.437	0.216	0.507	0.008	0.9446	0.17800	0.00102	2643	34	2634	10	-0.3
7991-58.1	311	143	0.47	183	12	0.00009	0.00003	0.00150	0.1361	0.0032	13.263	0.231	0.518	0.006	0.7945	0.18576	0.00198	2690	28	2705	18	0.6
7991-61.1	401	199	0.51	222	9	0.00006	0.00001	0.00097	0.1571	0.0024	11.579	0.146	0.483	0.005	0.9296	0.17398	0.00081	2539	23	2596	8	2.2
7991-73.1	1417	869	0.63	885	7	0.00001	0.00001	0.00019	0.1746	0.0007	13.819	0.157	0.532	0.006	0.9782	0.18824	0.00045	2752	24	2727	4	-0.9
03sb028A (Z7992)																						
7992-3.1	515	384	0.77	353	8	0.00003	0.00002	0.00059	0.2130	0.0022	16.166	0.190	0.560	0.003	0.6269	0.20945	0.00194	2866	14	2901	15	1.2
7992-18.1	670	29	0.04	393	1	0.00000	0.00001	0.00008	0.0116	0.0004	16.108	0.122	0.559	0.003	0.7195	0.20883	0.00111	2864	11	2896	9	1.1
7992-21.1	273	171	0.65	180	18	0.00014	0.00003	0.00236	0.1711	0.0025	16.071	0.239	0.556	0.003	0.4852	0.20960	0.00275	2850	13	2902	21	1.8
7992-37.1	389	1014	2.70	366	2	0.00001	0.00001	0.00019	0.7403	0.0029	16.108	0.137	0.560	0.003	0.6790	0.20868	0.00131	2866	12	2895	10	1
7992-42.1	373	215	0.60	250	1	0.00001	0.00001	0.00014	0.1661	0.0026	16.572	0.182	0.564	0.005	0.8519	0.21293	0.00123	2885	20	2928	9	1.5
7992-5.1	1154	87	0.08	676	433	0.00078	0.00006	0.01356	0.0281	0.0126	15.651	0.159	0.552	0.004	0.8152	0.20571	0.00122	2833	17	2872	10	1.4
7992-24.1	452	113	0.26	302	34	0.00015	0.00002	0.00257	0.0712	0.0010	19.190	0.155	0.595	0.004	0.8460	0.23379	0.00102	3011	15	3078	7	2.2

Notes (see Stern, 1997):
Uncertainties reported at 1s (absolute) and are calculated by numerical propagation of all known sources of error
$f206^{204}$ refers to mole fraction of total ^{206}Pb that is due to common Pb, calculated using the ^{204}Pb-method; common Pb composition used is the surface blank
* refers to radiogenic Pb (corrected for common Pb)
Discordance relative to origin = 100 * (1-($^{206}Pb/^{238}U$ age)/($^{207}Pb/^{206}Pb$ age))

Table 3. Summary of U-Pb age interpretations.

Unit	GSC Lab #	Sample #	UTM (zone 11; NAD 83)		Method	Mineral	Inter.	Age (Ma)	± 2S	Method	MSWD	Comment
			Easting	Northing								
Hickey pluton	z7992	03sb028	634180	7093818	TIMS	Zircon	Inh	>2855	-			2855–2970 age range
					TIMS	Monazite	IC	**2600.6**	**1.3**	WA	1.5	
					SHRIMP	Zircon	Inh	>2870				2870–3100 age range
Dauphinee pluton	z7990	03sb020	616604	7085037	TIMS	Zircon	IC	**2590**	**2.3**	WA	1.3	n=3
					SHRIMP	Zircon	IC	2591	3.6	WA	0.87	n=12
Armi pluton	z7988	03sb008	623526	7059544	TIMS	Zircon						discordant data; inheritance; no age interpretaton
					TIMS	Monazite						2568–2580 age range
					SHRIMP	Zircon	IC	**2600**	**5**	WA	0.23	n=10
Wecho pluton	z7991	03sb021	644660	7057428	TIMS	Monazite						2575–2580 age range
					SHRIMP	Zircon	IC	**2591**	**8**	WA	0.95	n=9

Interpretations: IC = igneous crystallization, Inh = inherited ages
Method: WA = weighted average; MSWD = mean square weighted deviates

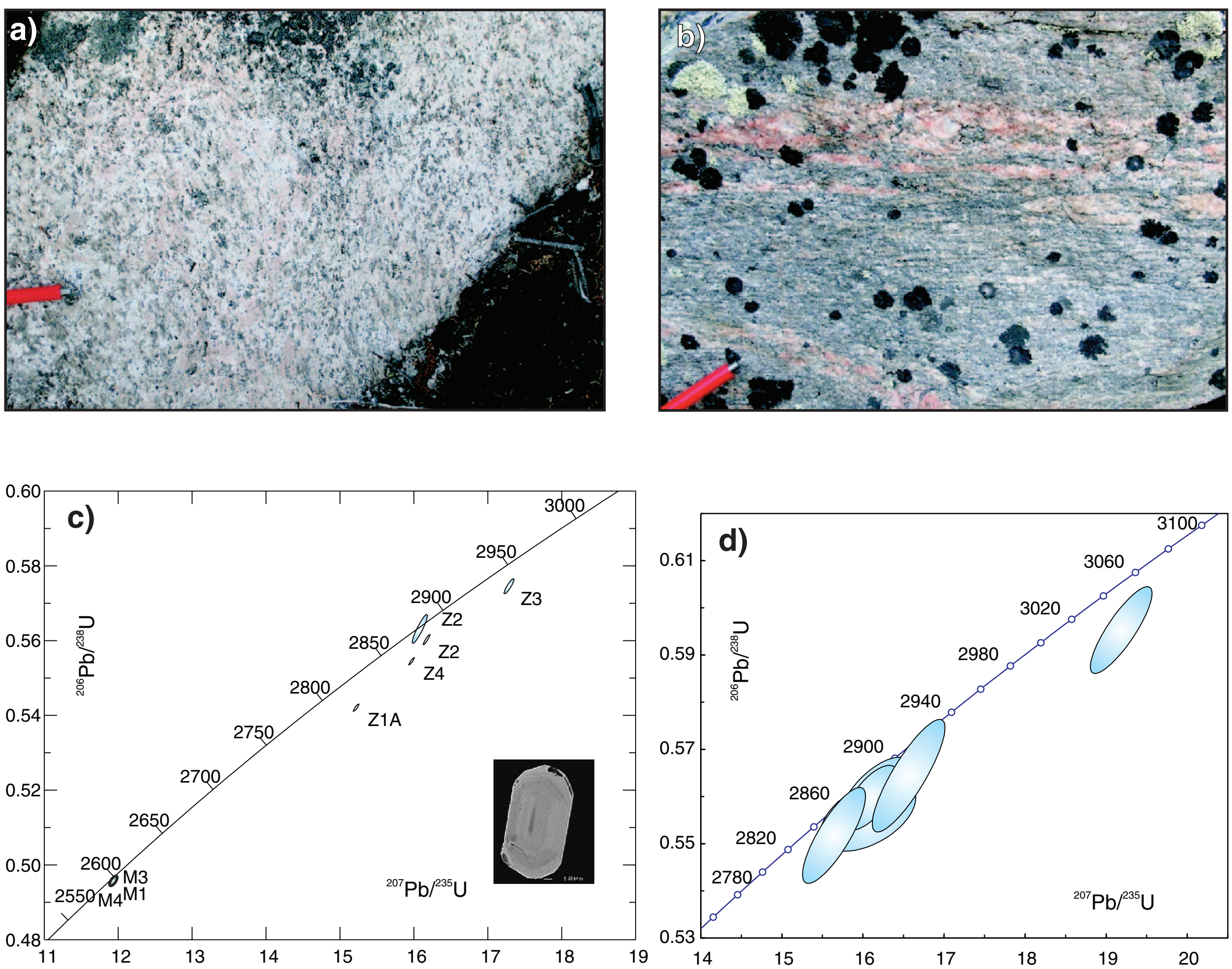

***Figure 3. a)** Outcrop photograph of Hickey pluton magnetite-bearing granite showing flattened quartz grains. **b)** Outcrop photograph of locally occurring gneissic phase near geochronological sample site. **c)** U-Pb concordia diagram showing results of TIMS analyses. Inset is backscattered electron image of zircon grain from the Z2 fraction. Z = zircon; M = monazite. **d)** Concordia diagram showing results of ion probe analyses. Blue ellipses represent inherited grains.*

with disseminated magnetite and biotite-rich knots, and contains variable amounts of compositionally layered mafic granulite enclaves. The recrystallized and extensively deformed nature of the pluton indicates that it likely intruded prior to, or synchronous with, granulite-grade metamorphism.

The physical characteristics of the pluton are similar to the oldest phase of the 2635 to 2600 Ma Disco suite in the neighbouring Snare River area (Jackson, 2003; Bennett et al., 2002) and parts of the approximately 2642 Ma Anton Suite from the Yellowknife area (Dudás et al., 1990). Gneissic phases within the map unit (Fig. 3b) appear similar to Mesoarchean basement exposures elsewhere in the southern part of the craton (Bleeker et al., 1999).

Results

This sample yielded monazite and zircon. Three different morphological types of monazite (Table 1) were identified and analyzed by TIMS, yielding reproducible ages with a weighted mean of 2600.6 ± 1.3 Ma (MSWD = 1.5)(Fig. 3c). Four principal zircon populations were identified: elongate prismatic grains (Z1); stubby prismatic grains (Z2); small, very clear prismatic to ovoid grains (Z3); and brownish, semi-prismatic grains (Z4). Backscatter electron images of the grains show that they are fractured, with some oscillatory zoning, but indicate no evidence of core-and-rim structures.

Four fractions, one single grain (Z2), two with four grains (Z3, Z4) and one with 7 grains (Z1), were analyzed by TIMS and yielded discordant ages between 2855 and 2970 Ma (Table 1; Fig. 3). Representative zircon grains were analyzed on the ion probe to determine the cause of this spread in ages and try to identify an igneous zircon growth event. Individual spot analyses of zircon grains range in age from 2.87 to 3.1 Ga and have variable Th/U ratios (Table 2). The majority of the grains have ages of about 2.9 Ga, but the range in ages do not define a single, statistically valid age population. This is supported by the large range in Th/U ratios indicating that the grains were not derived from a single magma composition. Consequently, both TIMS and ion probe results for the zircons are interpreted to reflect inheritance of zircon, rather than the timing of crystallization of the pluton. No evidence for zircon growth, either as distinct rims on inherited grains or new crystals was identified.

The reproducibility of the monazite ages is interpreted to represent one principal period of monazite growth. The authors suggest that the monazite age of 2600.6 ± 1.3 Ma is the best estimate for the timing of crystallization and that the zircons are inherited, with ages typical of the Central Slave Basement Complex (cf. Bleeker et al., 1999, and references therein).

Dauphinee pluton — enderbite (sample #03sb020 — lab #z7990)

Unit Description

The sample was collected to constrain the timing of granulite-grade metamorphism and the maximum age for late, non-charnokitic granites that extensively intrude this pluton. The Dauphinee pluton consists of charno-enderbite, enderbite, and mafic granulite (orthopyroxene-bearing granodiorite, tonalite, and quartz diorite, respectively) in the northern part of the study area (Fig. 2). The enderbite has a granofels structure and is heterogeneous, but generally plagioclase+hornblende+quartz+biotite+magnetite/ilmenite+clinopyroxene+orthopyroxene bearing (Fig. 4a, b); orthopyroxene occurs in the groundmass and locally in melt segregations. It is interpreted to have crystallized during granulite-grade metamorphism and is physically similar to a 2689 +1/-2 Ma orthopyroxene-bearing granodiorite from the neighbouring Wijinnedi area (Villeneuve and Henderson, 1998). Young, sheet-like porphyritic granite bodies extensively intrude the Dauphinee pluton, leaving most exposures on ridge tops. These topographic highs preserve the rocks as map-scale units, but it is unclear if the unit represents disrupted xenoliths entrained in the younger granite, or if it was intruded in place by the granites.

Results

Zircon in the sample is abundant and includes a variety of morphological types, ranging from light brown, stubby to elongate prisms, to large, brown and strongly corroded anhedral grains (Table 1). Backscatter electron images of the grains show they are altered and fractured. Five TIMS analyses of zircon have been completed, one multi-grain and four single grain, and the analyses plot in two groups on the Concordia diagram (Fig. 4c). The older grouping is characterized by dark brown, anhedral grains and includes one analysis of an elongate light brown prism. Although discordant, the three analyses have overlapping errors with a weighted mean $^{207}Pb/^{206}Pb$ age of 2590 ± 2.3 Ma (MSWD = 1.3) (Fig. 4c). This is interpreted as a minimum age for the rock. Two analyses of stubby, light brown to very clear prisms (Z1B, C) have younger $^{207}Pb/^{206}Pb$ ages with a weighted mean age of 2580 Ma (Fig. 4c). Due to the discordance in all the analyzed fractions, it is difficult to interpret the significance of the ages. The older date of 2590 Ma is a minimum age for crystallization of the pluton, whereas the younger fractions (Z1B, C) may reflect a period of later metamorphic growth or recrystallization. Alternatively, a maximum age can be estimated by regression of all five fractions, yielding an upper intercept of 2607 +18/-8 (lower intercept = 1962 Ma; MSWD = 0.36). Given that the analyses are tightly clustered and each cluster comprises different zircon morphological types, the latter interpretation is considered unlikely.

To evaluate the above interpretations, twelve analyses of unaltered, noncorroded zircon grains were completed on the ion probe (Table 2). These give a weighted mean age of 2591.9 ± 3.6 Ma (MSWD=0.87)(Fig. 4d) consistent with the weighted mean TIMS result. The age of the pluton is estimated to be 2590 ± 2.3 Ma. The origin of the discordance and younger approximately 2580 Ma ages for two TIMS fractions is not established.

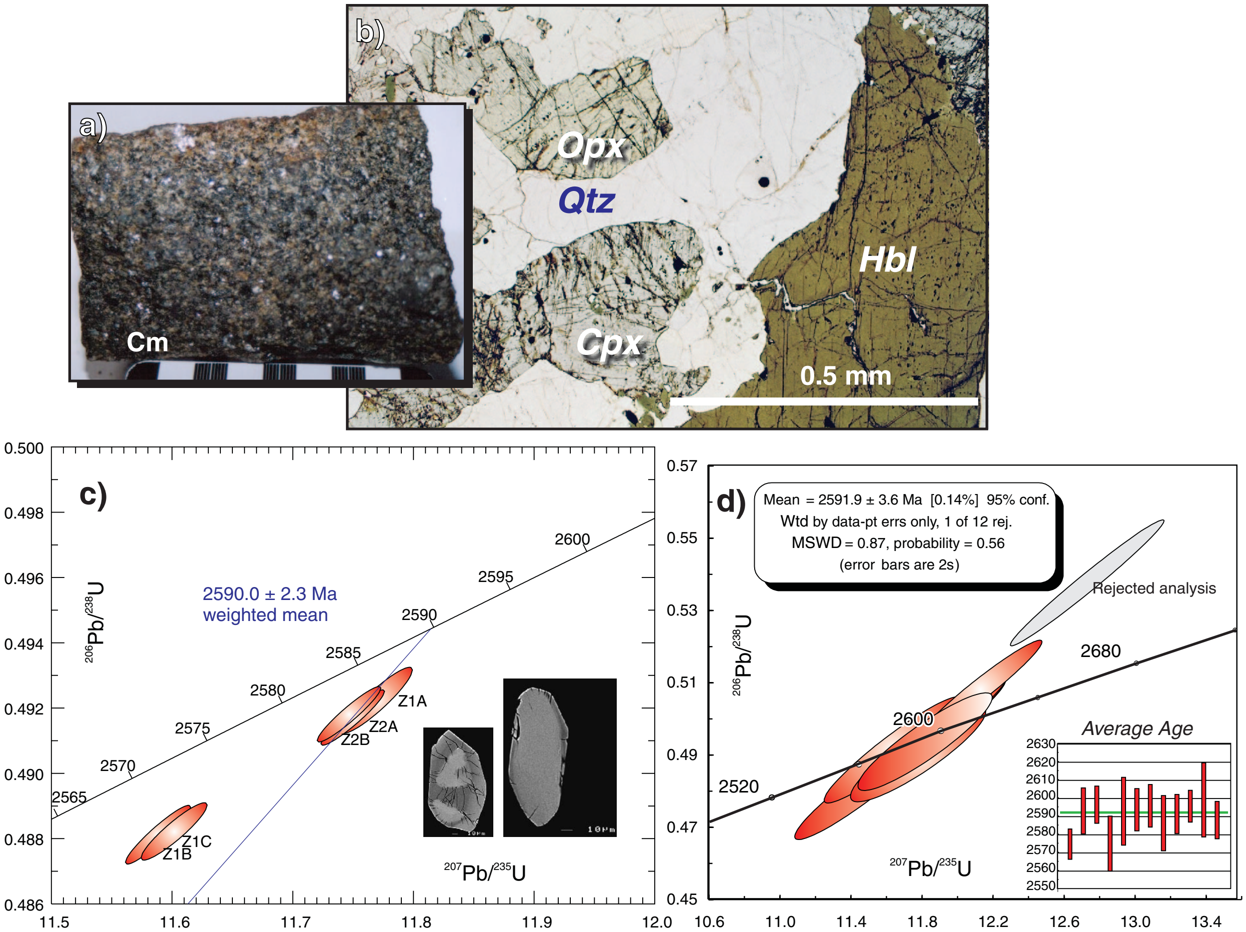

Figure 4. ***a)*** *Hand-sample photograph of hornblende-rich, orthopyroxene-bearing Dauphinee pluton enderbite.* ***b)*** *Photomicrograph of enderbite. Opx = orthopyroxene, Cpx = clinopyroxene, Hbl = hornblende, Qtz = quartz. Plane polarized light.* ***c)*** *U-Pb concordia diagram showing results of TIMS analyses. Inset is backscattered electron image of zircon grain from fraction Z1B on the right, showing alteration and fracturing, and on the left is an example of a large, corroded grain.* ***d)*** *Concordia diagram showing results of ion probe analyses. Z = zircon. Orange ellipses represent the crystallization ages of the zircons. One analysis was discarded due to its reverse discordance.*

Armi pluton — biotitegranodiorite (sample #03sb008 — lab #z7988)

Unit Description

The Armi pluton was sampled in order to constrain the maximum age of mid- to upper-amphibolite-grade metamorphism and associated deformation in the Armi Lake supracrustal belt (Fig. 2). The pluton is predominantly a medium-grained, equigranular granodiorite with minor amounts of primary and secondary muscovite. The pluton contains a moderate foliation defined by biotite. This foliation is coplanar with a foliation (defined by biotite, sillimanite, and melt) in the semi-pelitic rocks (Fig. 5a), as it can be traced through the pelitic rocks and across dykes that stem from the Armi pluton. The Armi pluton is interpreted to have intruded before or during S_2/S_3 development and related metamorphism.

Results

Zircon in this rock has four principal morphologies. Type Z1 consist of large, elongate, brown prismatic grains; Z2 comprise small, elongate, clear, colourless zircon; Type Z3 include intermediate-sized, stubby, prismatic varieties with very sharp terminations; and Z4 comprises smaller stubby prisms with well developed terminations. Backscatter electron images of the grains show complex zoning and alteration with some grains having core-rim structures. TIMS multi-grain analyses of three zircons from the Z2 fraction, and single-grain analyses of the Z1 and Z3 fraction, yield highly discordant ages (Fig. 5b). Ion probe analyses of ten zircons representing all four population types yielded a weighted mean age of 2600 ± 5 Ma (MSWD=0.23) (Fig. 5c), interpreted as the crystallization age of the Armi pluton. Two grains have older ages of 2701 and 2720 Ma (Table 2) and are interpreted to be inherited, as indicated by core-rim structures in BSE.

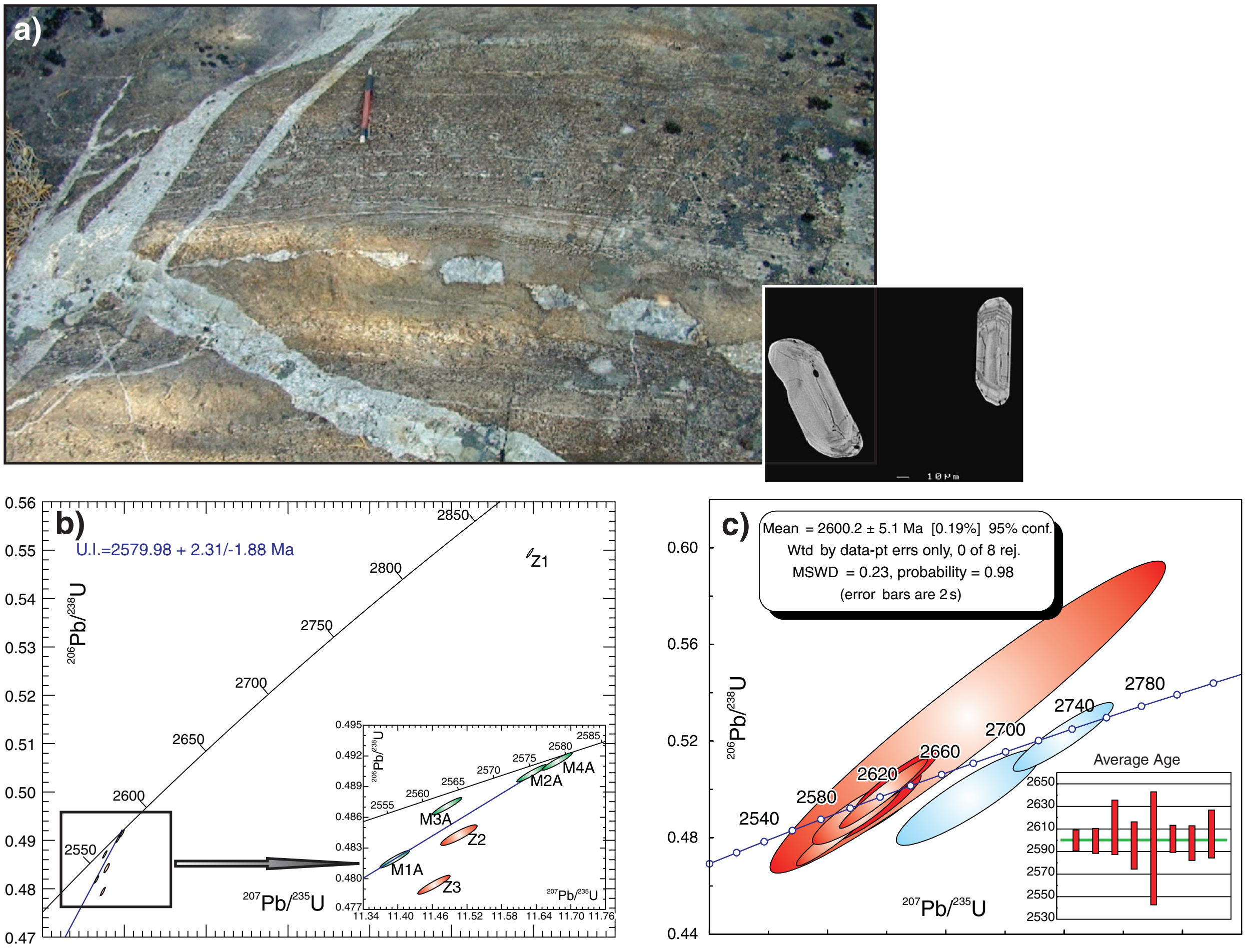

*Figure 5. **a)** Outcrop photograph showing Armi pluton biotite-granodiorite cutting pelitic rocks in the Armi Lake supracrustal belt. The granodiorite is boudinaged where it is parallel to the main foliation, which is defined by sillimanite + melt. Inset is an example of zircon population Z1 on the left, showing minor fracturing, and Z2 on the right showing complex zoning. **b)** U-Pb concordia diagram showing results of TIMS analyses. Z = zircon; M = monazite. **c)** Concordia diagram showing results of ion probe analyses. Orange ellipses represent the crystallization age of the zircons and blue ellipses represent inherited ages of the zircons.*

Three subtypes of monazite were identified in this sample and analyzed by TIMS (Table 1). The M1 variety is clear, pale, and subhedral. The second variety (M2/M3), comprise clear, pale yellow, but generally irregularly shaped crystals, often with broken edges. The third type (M4) is clear yellow, anhedral, and small. Six analyses were carried out and the results are variably discordant with $^{207}Pb/^{206}Pb$ ages between 2568 and 2580 Ma (Fig. 5b). The two oldest analyses (M2, M4) have ages of about 2580 Ma and are characterized by relatively low Th contents as indicated by $^{208}Pb/^{206}Pb$ ratios of about 10 (Table 1). The younger monazite ages are correlated with higher Th and $^{208}Pb/^{206}Pb$ ratios, suggesting that multiple generations of compositionally distinct monazite occur in this rock. The approximately 2570 Ma age of fraction M3A is an minimum estimate of the maximum age of the younger monazite generation. The 2580 Ma grains represent the minimum age of an older growth of monazite.

Wecho pluton (Stagg Suite?) — K-Feldspar Porphyritic Granite (Sample #03sb021 — lab #z7991)

Unit Description

The Wecho pluton was sampled to determine the age of the youngest magmatic event in the area and to constrain the maximum age of late deformation. The Wecho pluton is a K-feldspar porphyritic granite that occurs extensively throughout the study area as sheet-like intrusions (Fig. 2). This unit intrudes all other Archean rock types (Fig. 2, 6a) with the exception of an equigranular, two-mica granite. The relationship between these units is not observed. The pluton is biotite- and magnetite-bearing granite with K-feldspar phenocrysts up to 7 cm long (Fig. 6b). Muscovite is a secondary phase, occurring along fractures and grain boundaries. The pluton commonly displays a weak to moderate foliation defined by biotite and K-feldspar alignment. This foliation is locally folded. The Wecho pluton is physically similar to parts of the 2581 +29/-24 Ma Stagg Suite

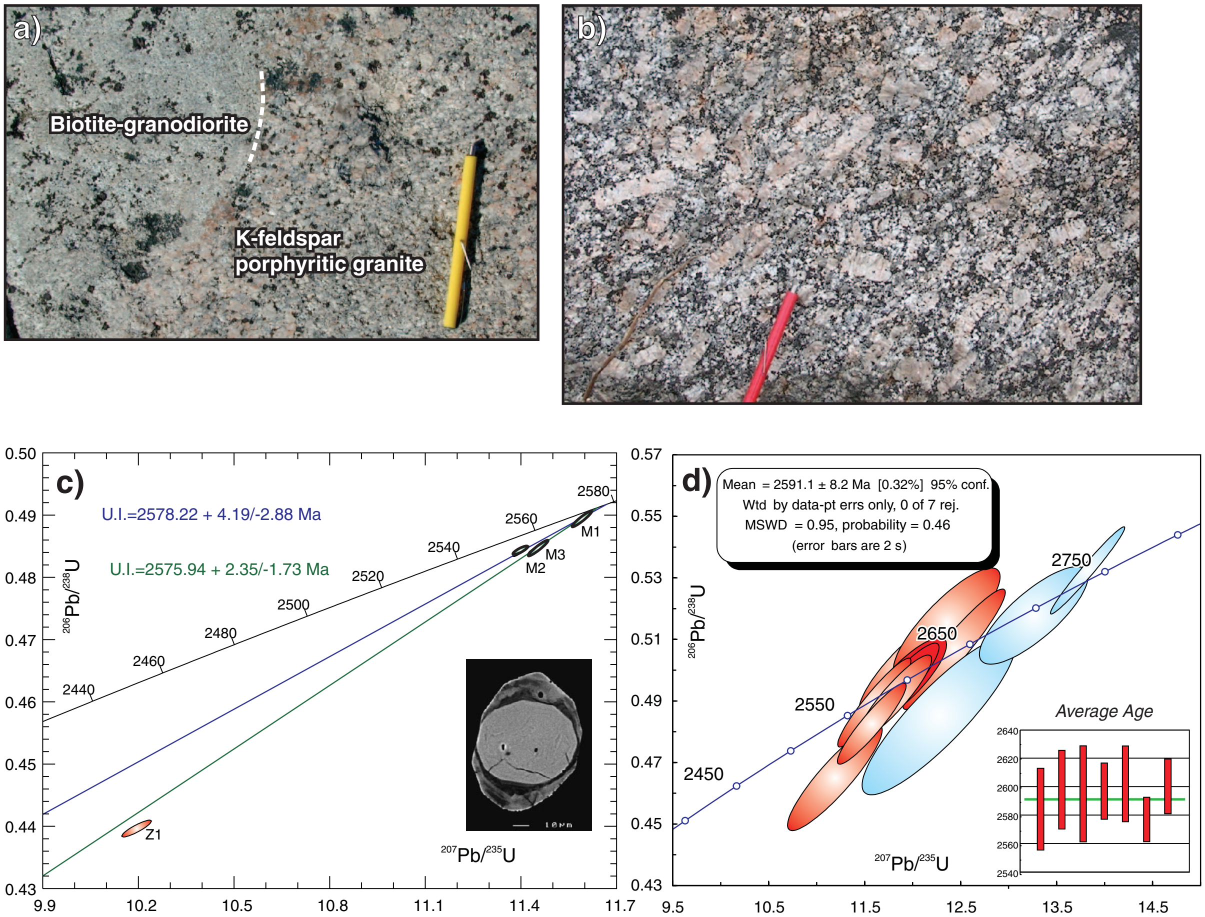

***Figure 6. a)** K-feldspar porphyritic granite intruding biotite-granodiorite. **b)** Outcrop photograph of the Wecho pluton K-feldspar porphyritic granite. **c)** U-Pb concordia diagram showing results of TIMS analyses. Inset is an example of zircon from the Z3 fraction exhibiting a core-rim structure with a re-crystallized rim. Z = zircon; M = monazite. **d)** Concordia diagram showing results of ion probe analyses. Orange ellipses represent the crystallization ages of the zircons. Blue ellipses represent inherited ages of the zircons.*

(Henderson, 1985; Henderson et al., 1987) and may be the upper-crustal equivalent to charnokitic, K-feldspar megacrystic granite described from the adjoining Snare River area to the west (Jackson, 2003).

Results

This sample contains a wide range of zircon morphological types. Backscatter electron images show many of the grains are highly altered and fractured with complex core-rim structures, in some cases indicative of inheritance. Three TIMS single-grain zircon analyses yield highly discordant ages (Table 1)(Fig. 6c). A weighted mean of 9 ion probe analyses, including both core and rim material, yielded an age of 2591 ± 8 Ma (MSWD=0.95)(Fig. 6d), and is interpreted here as the crystallization age of the pluton. Three other analyses yield ages of 2726 Ma (Table 2) and are interpreted as inherited.

Monazite grains from the sample are grouped into three morphologies (Table 1). M1 is well faceted, pale yellow, generally small, clear, and tabular. The second type (M2) is pale yellow, flat, and rounded. The third type (M3) is generally large blocky grains with irregular grain boundaries and shapes. The M2 and M3 types are slightly cloudy and this is reflected in greater discordance relative to M1. The three analyses do not define a single age population, but the M1 and M3 analyses have similar $^{207}Pb/^{206}Pb$ ages of about 2575 to 2580 Ma (Fig. 6c). For illustrative purposes, reference discordia lines are shown in Figure 6c that bracket this age range.

DISCUSSION

The U-Pb data for the Hickey pluton in the northern part of the study area indicate all zircons analyzed in this sample were inherited from Mesoarchean basement and the monazite data represent crystallization of the pluton at 2600.6 ± 1.3 Ma (Table 3). The age data indicate the pluton may be related to the youngest phase of the Disco suite to the west (Bennett et al., 2002), but likely not related to the 2642 Ma Anton Suite to the south (Dudás et al., 1990). The occurrence of inherited zircon (Table 3) demonstrates that Mesoarchean basement was present at the time of intrusion at about 2600 Ma in the northern part of the study area. The isotopic evidence presented here is the first indirect indication of Mesoarchean basement west of the Yellowknife Greenstone Belt and south of the Acasta Gneiss complex (Fig. 1; Bleeker et al., 1999). It is possible that the locally occurring gneissic unit in the Hickey pluton (Fig. 3b) may represent basement xenoliths, and the mafic granulite enclaves are remnants of an overlying mafic volcanic sequence. Sm-Nd isotopic work on similar samples throughout the study area will help delimit the extent of basement involvement in plutonism at approximately 2600 Ma.

The Dauphinee pluton enderbite yields a crystallization age of 2590 ± 2.3 Ma (Table 3). The crystallization age of the Dauphinee pluton, and previously discussed Hickey pluton, constrain the timing of granulite-grade metamorphism in the study area to younger than 2600 Ma and ongoing at 2590 Ma. Similarly, the timing of the 2590 Ma Dauphinee pluton and the 2589 Ma orthopyroxene-granodiorite from the Wijinnedi/Snare River area to the west (Villeneuve and Henderson, 1998), supports large-scale granulite-grade metamorphism in the northern part of the study area occurring after 2600 Ma and ongoing at approximately 2590 Ma, possibly concomitant with the onset of orogenic collapse as suggested by Bennett et al. (2002).

The crystallization age of ca. 2600 ± 5 Ma for the Armi pluton (Table 3) in the southern part of the study area provides a maximum age of upper-amphibolite-grade metamorphism and deformation in the Armi Lake supracrustal belt. The minimum age of a population of monazite at 2580 in the Armi pluton could also represent the extensive intrusion of late, two-mica granites into the area, a younger metamorphic event, or both (although the precise age of the younger granites is currently unknown). The monazite growth could be related to a relatively low-grade metamorphic event and concomitant formation of a crenulation cleavage, which is defined by biotite and locally muscovite, in the Armi Lake supracrustal belt. The maximum age of a monazite population at 2570 Ma is cryptic, but young ages are not unique and have also been identified in the eastern part of the craton by Schultz (2002) and in lower crust-derived granulite xenoliths by Davis et al. (2003).

The crystallization age of 2591 ± 8 Ma for the Wecho pluton (Table 3) is almost identical to the crystallization age of the granulite-grade Dauphinee pluton. The Wecho pluton is non-charnokitic and the assigned uncertainty of ±8 Ma allows for the pluton and associated rocks to be younger than the granulite-grade metamorphism. The monazite ages between 2575 and 2580 Ma likely represent post-crystallization growth, possibly during late deformation.

ACKNOWLEDGMENTS

We thank D. White and G. McKercher for their assistance during field mapping. The staff at the Geological Survey of Canada's J.C. Roddick Ion Microprobe (SHRIMP) Laboratory provided assistance and expertise. Ongoing discussions with V.A. Jackson, V. Bennett, W. Bleeker, and M. Stubley have greatly improved our knowledge of the region. Figure 1 is used courtesy of W. Bleeker. Thoughtful reviews by E. Martel, W. Bleeker, O. van Breemen, and V.A. Jackson improved the manuscript. A Government of the Northwest Territories, Department of Education, Culture and Employment internship for L. Ootes is acknowledged. Northwest Territories Geoscience Office Contribution Number 0013.

REFERENCES

Bennett, V., Rivers, T., and Relf, C.
2002: Where east meets west: formation, growth, and collapse of the Snare River terrain, southwestern Slave Province; Program of Abstracts, 30th Yellowknife Geoscience Forum, Yellowknife, Northwest Territories, p. 1–2.

Bleeker, W. and Davis, W.J.
1999: The 1991-1996 NATMAP Slave Province project: introduction; Canadian Journal of Earth Sciences, v. 36, p. 1033–1042.

Bleeker, W., Ketchum, J.W.F., Jackson, V.A., and Villeneuve, M.E.
1999: The Central Slave Basement Complex, Part I: its structural topology and autochthonous cover; Canadian Journal of Earth Sciences, v. 36, p. 1083–1109.

Cumming, G.L. and Richards, J.R.
1975: Ore lead isotope ratios in a continuously changing Earth; Earth and Planetary Science Letters, v. 28, no. 2, p. 155–171.

Davis, W.J. and Bleeker, W.
1999: Timing of plutonism, deformation, and metamorphism in the Yellowknife Domain, Slave Province, Canada; Canadian Journal of Earth Sciences, v. 36, p. 1169–1187.

Davis, W.J. and Hegner, E.
1992: Neodymium isotopic evidence for the tectonic assembly of Late Archean crust in the Slave Province, northwest Canada; Contributions to Mineralogy and Petrology, v. 111, p. 493–504.

Davis, W.J., Canil, D., MacKenzie, J.M., and Carbno, G.B.
2003: Petrology and U–Pb geochronology of lower crustal xenoliths and the development of a craton, Slave Province, Canada; Lithos, v. 71, p. 541–573.

Davis, W.J., Gariépy, C., and van Breemen, O.
1996: Pb isotopic composition of late Archaean granites and the extent of recycling early Archaean crust in the Slave Province, northwest Canada; Chemical Geology, v. 130, p. 255–269.

Dudás, F.Ö., Henderson, J.B., and Mortenson, J.K.
1990: U-Pb ages of zircons from the Anton Complex, southern Slave Province, Northwest Territories; Geological Survey of Canada, Paper 89-2, p. 39–44.

Henderson, J.B.
1985: Geology of the Yellowknife-Hearne Lake area, District of Mackenzie: a segment across an Archean basin; Geological Survey of Canada, Memoir 414, 135 p.
2004: Geology of the Wijinnedi Lake area, Northwest Territories; Geological Survey of Canada, Bulletin 576, 115 p.

Henderson, J.B., van Breemen, O., and Loveridge, W.D.
1987: Some U-Pb zircon ages from Archean basement, supracrustal and intrusive rocks, Yellowknife-Hearne Lake area, District of Mackenzie; Geological Survey of Canada, Paper 87-2, p. 111–121.

Jackson, V.J.
2003: Preliminary compilation of the geology of the Snare River (1998-2002 results), Wijinnedi Lake, Labrish Lake, and Russell Lake areas; parts of 85O and 85N; C.S. Lord Northern Geoscience Centre, Northwest Territories Open File 2003-002, 1 map, scale 1:100 000.

Ludwig, K.R.
2003: User's manual for Isoplot/Ex rev. 3.00: a geochronological toolkit for Microsoft Excel; Berkeley Geochronology Center, Berkeley, California, Special Publication, 4, 70 p.

MacLachlan, K., Davis, W.J., and Bleeker, W.
2002: Distribution of Mesoarchean crust in the southern Slave Province as revealed by the Nd and Pb isotopic composition of ca. 2.6 Ga granites; Program of Abstracts, 30th Yellowknife Geoscience Forum, Yellowknife, Northwest Territories, p. 42–43.

Ootes, L.
2004: Geology of the northern part of the Wecho River area, NTS 85O-9, 10, 15, and 16; C.S. Lord Northern Geoscience Centre, Northwest Territories Open File 2004-003, 2 maps, scale 1:100 000.

Parrish, R.R., Roddick, J.C., Loveridge, W.D., and Sullivan, R.W.
1987: Uranium-Pb analytical techniques at the geochronology laboratory, Geological Survey of Canada; Geological Survey of Canada, Paper 87-2, p. 3–7.

Padgham, W.A. and Fyson, W.K.
1992: The Slave Province: a distinct Archean craton; Canadian Journal of Earth Sciences, v. 29, p. 2072–2086.

Pehrsson, S.J.
2002: Geology, Indin Lake, Northwest Territories; Geological Survey of Canada, Open File 4268, scale 1:125 000.

Roddick, J.C.
1987: Generalized numerical error analysis with applications to geochronology and thermodynamics; Geochimica et Cosmochimica Acta, v. 51, p. 2129–2135.

Roddick, J.C., Loveridge, W.D., and Parrish, R.R.
1987: Precise U-Pb dating of zircon at the sub-nanogram Pb level; Chemical Geology, v. 66, p. 111–121.

Schultz, M.
2002: Th-U-total Pb dating of a polygenetic late Archean terrane: Walmsley Lake area, NTS 75N; Program of Abstracts, 30th Yellowknife Geoscience Forum, Yellowknife, Northwest Territories, p. 56.

Stern, R.A.
1997: The GSC Sensitive High Resolution Ion Micro Probe (SHRIMP): analytical techniques of zircon U-Th-Pb age determinations and performance evaluation; Geological Survey of Canada, Current Research 1997-F, p. 1–31.

Stern, R.A. and Amelin, Y.
2003: Assessment of errors in SIMS zircon U-Pb geochronology using a natural zircon standard and NIST SRM 610 glass; Chemical Geology, v. 197, p. 111–146.

Stubley, M.P.
1997: Geological compilation of the Carp Lakes area; NTS 85P and southeastern 85O; Indian and Northern Affairs Canada, Northwest Territories, Geology Division, EGS 1997-07, 1 map, scale 1:250 000.

Thorpe, R.I., Cunningham, G.L., and Mortensen, J.K.
1992: A significant Pb isotope boundary in the Slave Province and its probable relation to ancient basement in the western Slave Province; in, Project Summaries: Canada - Northwest Territories Mineral Development Subsidiary Agreement, 1987–1991, Geological Survey of Canada, Open File 2484, p. 179–184.

Villeneuve, M.E. and Henderson, J.B.
1998: U-Pb geochronology of the Wijinnedi Lake area, Slave Province, District of Mackenzie, Northwest Territories; Geological Survey of Canada, Current Research 1998-F, p. 99–106.

Yamashita, K., Creaser, R.A., Stemler, J.U., and Zimaro, T.W.
1999: Geochemical and Nd-Pb isotopic systematics of late Archean granitoids, southwestern Slave Province, Canada: constraints for granitoid origin and crustal isotopic structure; Canadian Journal of Earth Sciences, v. 36, p. 1131–1147.

Yardley, D.H.
1949: Preliminary map: Wecho River (east half), Northwest Territories; Geological Survey of Canada, Paper 49-14, scale 1 inch: 2 miles.

York, D.
1969: Least squares fitting of a straight line with correlated errors; Earth and Planetary Science Letters, v. 5, p. 320–24.

Geological Survey of Canada Project Y04